

MODELLING OF POWDER FLOW IN ROTATIONAL MOULDING

R. Pantani, M. d'Amore, G. Titomanlio

Department of Chemical and Food Engineering, University of Salerno, Fisciano (SA), Italy

R. Mauri,

Department of Chemical Engineering, The City College of CUNY, New York, NY 10031

Rotational moulding is a widely used technological process to obtain hollow plastic articles, in which polymer powders melt within a rotating mould. The first step in modelling the melting process is to analyse the kinematics of the powder in the rotating system. To this goal, a series of experimental observations was performed on a rotating cylinder partially filled with a powder (Sand X, average size 460 microns) with known physical characteristics (such as angles of repose and angles of approach). A phenomenological model was then developed, based on the assumption that the powder behaves as a Bingham-plastic fluid, obtaining theoretical predictions which were in good agreement with the experimental measurements.

keywords: Rotational moulding, powders, fluid dynamics, rotating cylinder

INTRODUCTION

Rotational moulding is a widely used technology to manufacture hollow industrial products. In this process, a thermoplastic powder is rotated in an oven around two perpendicular axes, so that the powder eventually melts and adheres to the internal surface of the mould.

The different stages of the process are schematized in Figure 1. The apparatus is composed of two axes, allowing double rotation of the mould. Concretely, the process is divided into three stages:

1. The mould is cleaned and filled with powder. Then, the mould is rotated along the two axes, so that the powder distributes uniformly on the inner surface of the mould.
2. The rotating mould is introduced in an oven, kept at constant temperature, where the powder melts. An important condition to obtain a high-quality product is that the powder is heated homogeneously, which in turn requires a uniform powder distribution.
3. The mould is cooled down, until the fluid solidifies.

From this description, it is apparent that in order to improve the quality of the product, a better understanding of the heat and mass transport during the process is required.

Due to the intrinsic difficulty of the powder fluid dynamics inside the chamber, approximations are made in the existing models. In fact, current modelling of the powder flow assumes that the powder in contact with the rotating mould is static relative to the mould wall; that the powder being released from the mould surface falls on the static powder without exchange of material (e.g. it is freely falling); and that during free fall the temperature profile of the powder upon contact with the mould surface is flat [1].

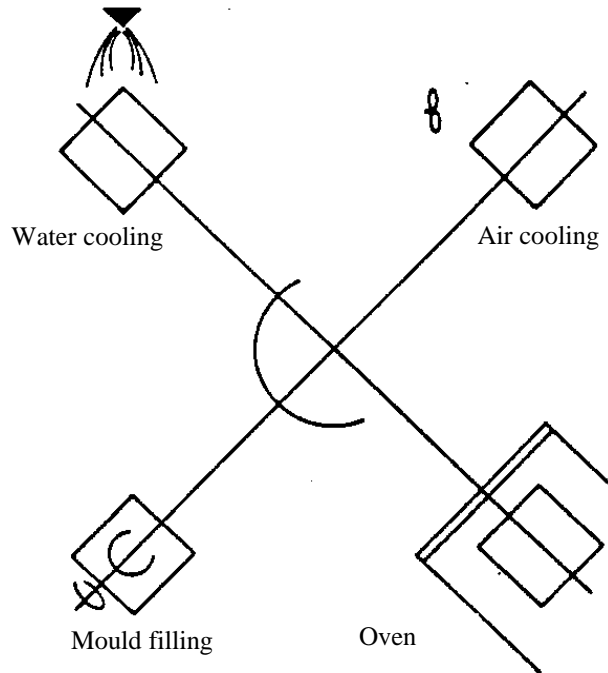


Figure1: *Typical rotational moulding apparatus*

Aim of this work is to shed some light on the mechanism of the powder flow inside the mould. For a preliminary analysis of the system, it is advisable to study the simplest possible mould shape. The first step in modelling the process is to study the movement of the powder in the system. Also a complete knowledge of the characteristics of the powder flowing in the mould is needed.

In the work, a series of experimental observations was performed using a rotating Pyrex cylinder partially filled with a powder of known characteristics. Images taken with a camera were computer analysed by means of an image acquisition system. A phenomenological model was then developed.

EXPERIMENTAL

A cylinder (0.14m in diameter, 0.4m long) having Pyrex surfaces was partially filled with 400mL of sand whose physical characteristics are shown in Table 1. This sand is a type B powder in the Geldart's classification so that short-range interparticle forces are small and the study of the powder dynamics is easier.

TABLE 1: physical characteristics of the sand used in our experiments.

Material	Particle size [microns]	Bulk density [gm/cm³]	Angle of repose* (α)	Angle of approach* ($90^\circ - \beta$)
Rounded sand	380~540	1.6	35°	46°

* with respect to the horizontal

The cylinder rotational velocity was ensured by a computer controlled 500 W electrical engine. The velocity could be varied from 5 to 100 rpm. Images were taken by both a photcamera for snapshooting the flow lines of the powder (exposing time 1/500 s), and a digital high resolution videocamera for powder motion processing. This latter was computer-aided so as to have possibility of measuring the velocity of single particles.

At very low rotation speed, the material was raised beyond its angle of repose, subsequently collapsing to a lower angle. Then, increasing the speed up to 30rpm, the surface

became substantially steady (Fig.2) and the measured angle of elevation of this surface was close to the angle of repose of the powder. Finally, at higher speeds (still lower than the critical speed at which centrifugal forces predominates on gravity forces) the free surface assumed an elongated S-shape (Fig.3). The measured angle at the steepest part of this surface resulted to be close to the angle of approach.

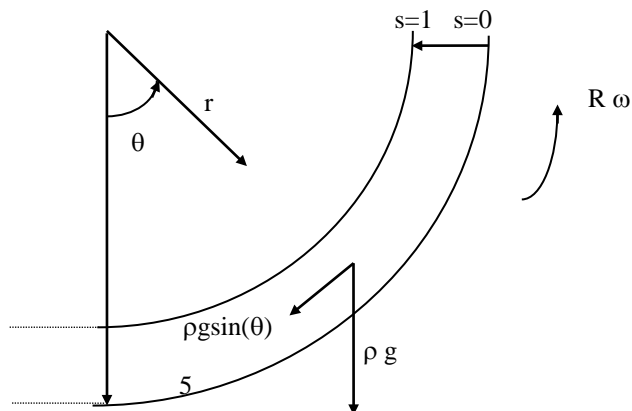
Figure 2. *Experimental observation of the powder profile during rotation in the cylinder. Material: Sand X, $\omega=30\text{rpm}$, $R=7\text{cm}$, $L=40\text{cm}$, Volume of powders= 400cm^3*

As shown in figures 2 and 3, three zones can be clearly distinguished: a top zone of rapidly flowing powder; a middle zone in which the material is substantially steady; a bed of material rotating with the cylinder. A similar zone division is observed if the layer of powder is thinner, although at very high speeds the surface is not perfectly identifiable.

Figure 3. *Experimental observation of the powder profile during rotation in the cylinder. Material: Sand X, $\omega=60\text{rpm}$, $R=7\text{cm}$, $L=40\text{cm}$, Volume of powders= 400cm^3*

THEORETICAL ANALYSIS

It is well known that granular materials can flow like liquids, and there is a variety of theoretical models used to describe such flows (see Jaeger *et al.*, 1996, and references herein).



$$r = R-d$$

$$r = R$$

Figure 4: *Schematics of the rotating cylinder.*

In particular, for simple geometries such as ours, it is known that powders can be modelled as Bingham plastic fluids (Rietema, 1991). Therefore, assuming that the motion of the powder takes place within a thin layer of thickness $d \ll R$ (see Figure 4), with $d/dr \gg d/(R\theta)$, at leading order the equation of motion can be written in terms of the non-dimensional distance s from the wall,

$$r = R \left(1 - s \frac{d}{R} \right), \quad (1)$$

as:

$$\frac{d\tau}{ds} = -\rho dg \sin \theta, \quad (2)$$

where g is the gravity field and τ the shear stress. In this approximation we have assumed that the width L of the cylinder is large, so that edge effects can be neglected and the motion of the powder, at leading order, can be assumed to be one-dimensional, along the circumferential direction. Equation (2) can be easily integrated, since $\tau = 0$ at $s = l$, so that we obtain:

$$\tau = \rho dg \sin \theta (1 - s). \quad (3)$$

The shear stress is given by the Bingham expression,

$$\begin{aligned} \tau &= \tau_0 - \frac{\mu}{d} \left(\frac{dv}{ds} \right) \quad \text{if } |\tau| \geq \tau_0 \\ \frac{dv}{ds} &= 0 \quad \text{if } |\tau| < \tau_0 \end{aligned} \quad (4)$$

where v is the velocity in the circumferential direction, while τ_0 and μ are constant Bingham parameters. At this point, we have to impose the boundary condition at the wall. Now, in general, powders tend to slip, depending on the coarseness of both powder and wall, and on the local pressure field. However, for lack of experimental data, here we have assumed that the wall is sufficiently coarse to allow the no-slip boundary condition to be satisfied, i.e. $v(s=0) = v_w = \omega R$, obtaining,

$$\begin{aligned} v &= \omega R \left[1 - A s_0^2 \left(2 \frac{s}{s_0} - \frac{s^2}{s_0^2} \right) \right] \quad \text{for } s < s_0 = 1 - \frac{\tau_0}{\rho dg \sin(\theta)}; \\ v &= \omega R [1 - A s_0^2] \quad \text{for } s > s_0 = 1 - \frac{\tau_0}{\rho dg \sin(\theta)}, \end{aligned} \quad (5)$$

where

$$A = \frac{\rho d^2 g \sin(\theta)}{2\omega R \mu}$$

represents the ratio between the free-fall velocity of the powder layer and its imposed velocity at the walls, while

$$s_0 = 1 - \frac{\tau_0}{\rho d g \sin(\vartheta)}$$

is the distance from the wall at which we start to observe plug flow. Note that, in order to find an upper layer of particles falling under the influence of gravity, we must have $As_0^2 \geq 1$.

In addition, there is an additional condition to be satisfied, stating that since the powder is incompressible, its total volume is constant and equal to V . Therefore, imposing that the volumetric flux is zero at each angle, i.e.,

$$Q = Ld \int_0^1 v ds = LdR\omega \left[1 - As_0^2 \left(1 - \frac{1}{3}s_0 \right) \right] = 0, \quad (6)$$

we easily find $d = d(\vartheta)$, representing the thickness of the powder layer along the circumference.

The analytical solution (equation 5) can also be used to determine the position within the powder layer at which the powder velocity is zero, finding,

$$s^* = s_0 \left[1 - \sqrt{1 - \frac{1}{As_0^2}} \right]. \quad (7)$$

This curve $s^*=s^*(\theta)$ represents the separating line between the upper region, with positive velocities, and the lower region, with negative, gravity-driven, velocities.

In order to compare the predictions of this model with our experimental results, we have chosen the following values of the physical parameters:

$$\tau_0 = 257 \frac{\text{dyne}}{\text{cm}^2}; \quad \mu = 416p; \quad \rho = 1.6 \frac{\text{g}}{\text{cm}^3}; \quad (8)$$

$$L = 40\text{cm}; \quad R = 7\text{cm}; \quad d \approx 2\text{cm}; \quad \omega = 0.5\text{Hz}; \quad V = 400\text{cm}^3.$$

where the Bingham parameter τ_0 was determined from independent measurements of the angle of repose, while μ was fitted comparing our theoretical predictions of the zero-velocity curve (equation 7) with our experimental measurements.

Our analytical solution (equation 5) shows that when $s_0=0.9$ and $A=1.76$ (which turns up to correspond to an angular position $\theta=55^\circ$, i.e. the bed of powder is at its angle of repose respect to the horizontal), the powder rotates together with the cylinder near the cylinder wall, while at the edge of the powder layer it moves in the opposite direction, falling under gravity, with a zero-velocity curve located at $s=0.4$ (see Figure 5).

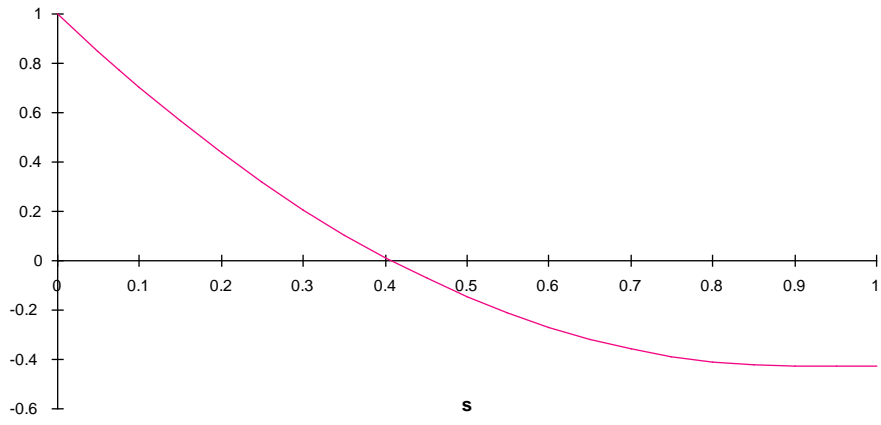


Figure 5. Typical velocity profile, $v/(\omega R)$, at a fixed angular position, $\theta=55^\circ$, corresponding to the powder repose angle.

Substituting the values (equation 8) of the physical parameters into Eq. (6), we find the thickness of the powder layer, plotted in Figure 6.

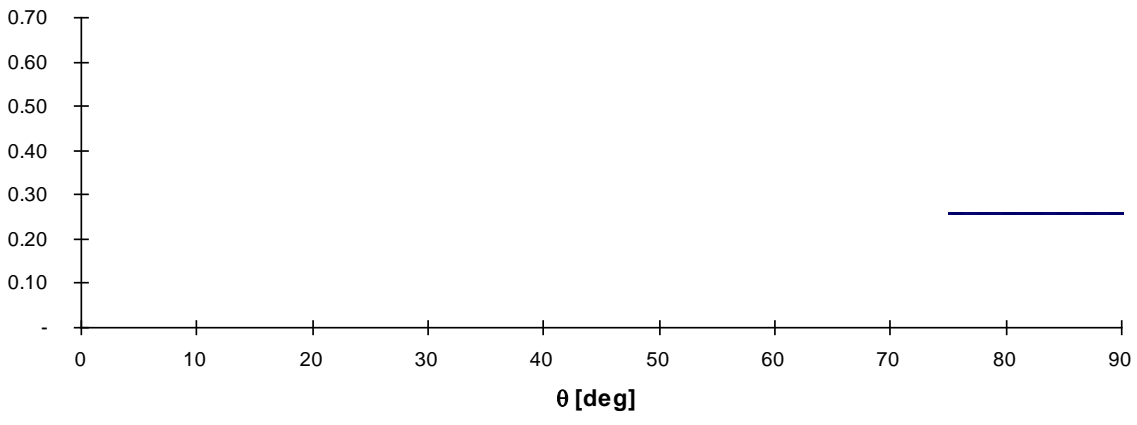


Figure 6: Thickness of the powder layer $d=d(\theta)$.

Finally, plotting equation (7), we obtain the curve of figure 7, separating the upper region, with positive velocities, from the lower region, with negative, gravity-driven, velocities.

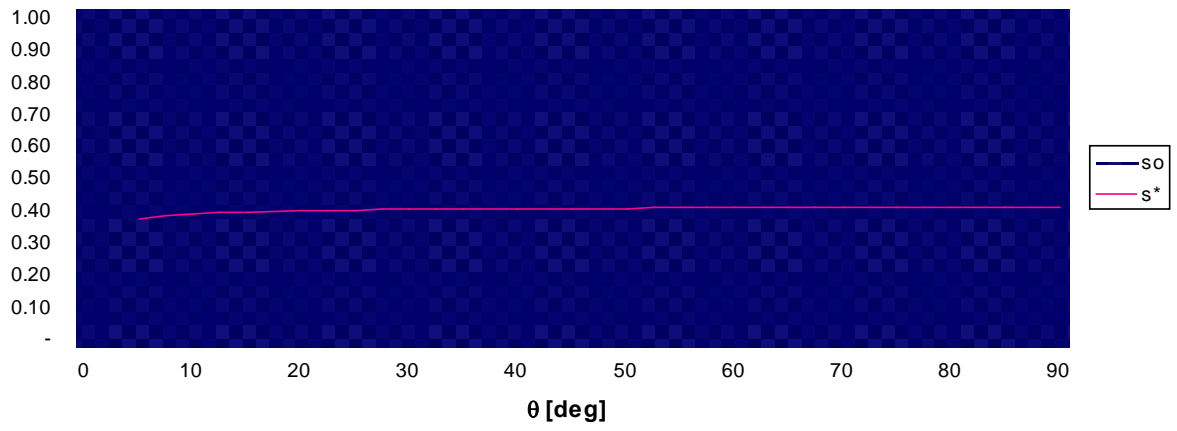


Figure 7: Profile of the curve $s=s(\theta)$ separating the region with positive velocities from that of negative velocities.

Bibliography

- Brown and Richards, *Principles of Powder Mechanics*, Pergamon Press, New York (1966).
- Jaeger, H.M., S.R. Nagel and R.P. Behringer, Granular solids, liquids and gases, *Rev. Mod. Phys.* **68**, 1259 (1996).
- Marchello and A. Gomezplata, *Gas-Solid Handling in the Process Industry*, Marcel Dekker, NewYork (1976).
- Rietema, K., *The Dynamics of Fine Powders*, Elsevier, London, 1991(1991).
- Suzuki and Tanaka, “Measurement of Flow Properties of Powders along an Inclined Plane”, *Ind. Eng. Chem. Fundam*, **10**, 84 (1971).
- Throne, *Plastic Process Engineering*, UMI (1994).
- Titomanlio, Stampaggio Rotazionale, CLUP (1988).